Electronic Supplementary Information for

Ultrafast Photo-driven Charge Transfer Exciton Dynamics in Mixed-Stack Pyrene-Perylenediimide Single Co-crystals

Michele S. Myong, Yue Qi, Charlotte Stern, and Michael R. Wasielewski*

Department of Chemistry and Institute for Sustainability and Energy at Northwestern,

Northwestern University, Evanston, IL 60208-3113

Table of Contents

Section 1: Crystal Growth and Structure Determination **2**
Section 2: Steady-state Absorption and Emission Microscopy **6**
Section 3: Femtosecond Transient Absorption Microscopy **13**
Section 4: Calculation of excitation density **14**
Section 5: Calculation of diffusion coefficients **15**
References **17**

Section 1: Crystal Growth and Structure Determination

Crystal growth

The Pyr-C_5PDI co-crystal was grown from 4 mL of 3.75 mM pyrene and 3.75 mM C_5PDI in $CHCl_3$. This solution was pipetted into culture tubes (Fisher brand, 6×50 mm lime glass), which were placed in a 20 mL glass vial filled with ~8 mL of MeOH, and the single co-crystals were grown by vapor diffusion. Similarly, the Pyr-diisoPDI co-crystal was grown from 4 mM pyrene and 4 mL of 4 mM diisoPDI in $CHCl_3$ using the same techniques. Once the crystals were visible by eye, they were drop cast from the mother solution onto a glass slide and the solvent was allowed to evaporate.

Single Crystal X-ray Diffraction

A suitable single crystal of Pyr-C_5PDI with dimensions of 0.049×0.071×0.268 mm^3 was mounted on a loop with paratone oil on an XtaLAB Synergy diffractometer equipped with a micro-focus sealed X-ray tube PhotonJet (Cu) X-ray source and a Hybrid Pixel Array Detector(HyPix) detector. The temperature of the crystal was controlled at 100.0 K with an Oxford Cryosystems low-temperature device. Data reduction was performed with CrysAlisPro software using an empirical absorption correction. The crystal under investigation was found to be non-merohedrally twinned. The orientation matrices for the two components were identified using the program CrysAlisPro (Rigaku Oxford Diffraction, 2019). The exact twin matrix identified by the integration program was found to be (-0.9996 0.0001 -0.0007 -0.0023 -0.9991 0.0022 -0.4445 -0.0238 1.0001). The second domain is rotated from first domain by -179.9126% about the reciprocal lattice c axis. An hklf5 file was used in all refinements. The structure was solved using direct methods with only the non-overlapping reflections of component 1. The twin fraction refined to a value of 0.413(2).The structure was solved using the XS[1] structure solution program using direct methods and by using Olex2[2] as the graphical interface. The model was refined with

the XL^3 refinement package using Least Squares minimization. The final structure has been submitted to the Cambridge Crystallographic Data Centre: CCDC 2092900.

Crystal Structure Data for Pyr-C_5PDI:$C_{100}H_{80}N_4O_8$ (M =1437.75 g/mol): triclinic, space group P-1 (no. 2), a = 7.3795(10) Å, b = 9.5328(2) Å, c = 26.1396(6) Å, α = 89.271(2)°, β = 86.498(2)°, γ = 84.068(2)°, V = 1825.55(6) Å^3, Z = 1, T = 100.0 K, μ(CuKα) = 0.7659 mm^{-1}, *Dcalc* = 1.333 g/cm^3, 10696 reflections measured (6.776° ≤ 2Θ ≤ 155.016°), 7547 unique (R_{int} = merged, R_{sigma} = 0.0075) which were used in all calculations. The final R_1 was 0.0901 (I > 2σ(I)) and wR_2 was 0.2825 (all data).

A suitable single crystal of Pyr-diisoPDI with dimensions of 0.064×0.098×0.255 mm^3 was mounted on a loop with paratone oil on the diffractometer system described above, and the diffraction data was collected at 100.1 K. The structure was solved as described above for the Pyr-C_5PDI crystal. Squeeze was used to remove disordered chloroform solvent molecules. The pyrene moiety (C48-63) displayed disorder and was modeled over two positions. Restraint RIGU was applied to moiety C48-C63 and C48A-C63A. The final structure has been submitted to the Cambridge Crystallographic Data Centre: CCDC 2092901.

Crystal Structure Data for Pyr-diisoPDI: $C_{64}H_{51}N_2O_4$ (M = 912.07 g/mol): monoclinic, space group $P2_1/c$, a = 8.6684(3) Å, b = 19.1525(5) Å, c = 30.3884(8) Å, α = 90°, β = 92.739(3)°, γ = 90°, V = 5039.4(3) Å^3, Z = 4, T = 100.0 K, μ(CuKα) = 0.648 mm^{-1}, *Dcalc* = 1.202 g/cm^3, 32028 reflections measured (7.432° ≤ 2Θ ≤ 153.554°), 10136 unique (R_{int} = 0.0329, R_{sigma} = 0.0249) which were used in all calculations. The final R_1 was 0.1070 (I > 2σ(I)) and wR_2 was 0.3059 (all data).

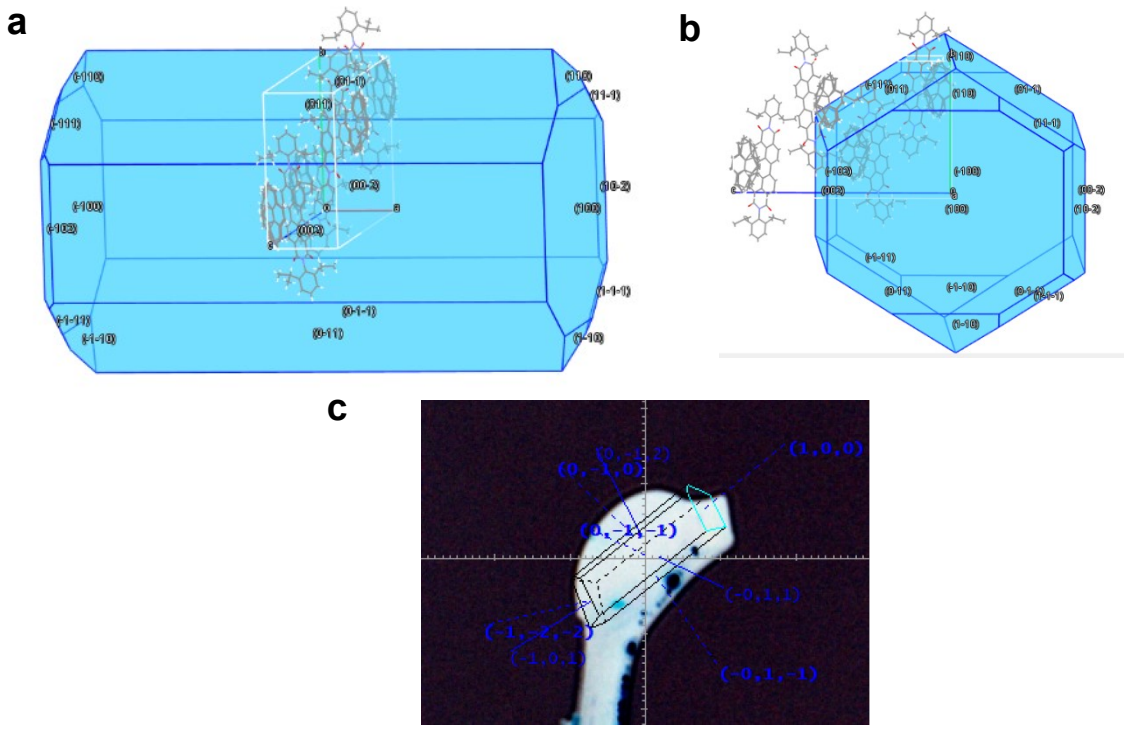

Figure S1: BFDH calculations were completed in Mercury for Pyr-diisoPDI co-crystal. (a) View of the crystal along the (002) axis shows the molecules stack with their transition dipole moments perpendicular to the long axis of the crystal. (b) View of the crystal along the (100) axis shows a degree of interstack overlap, though the planes of the molecules are not perfectly cofacial with the axis of the crystal. (c) Manual face indexing of the mounted single crystal that was diffracted shows reasonable agreement with the BFDH calculated structures.

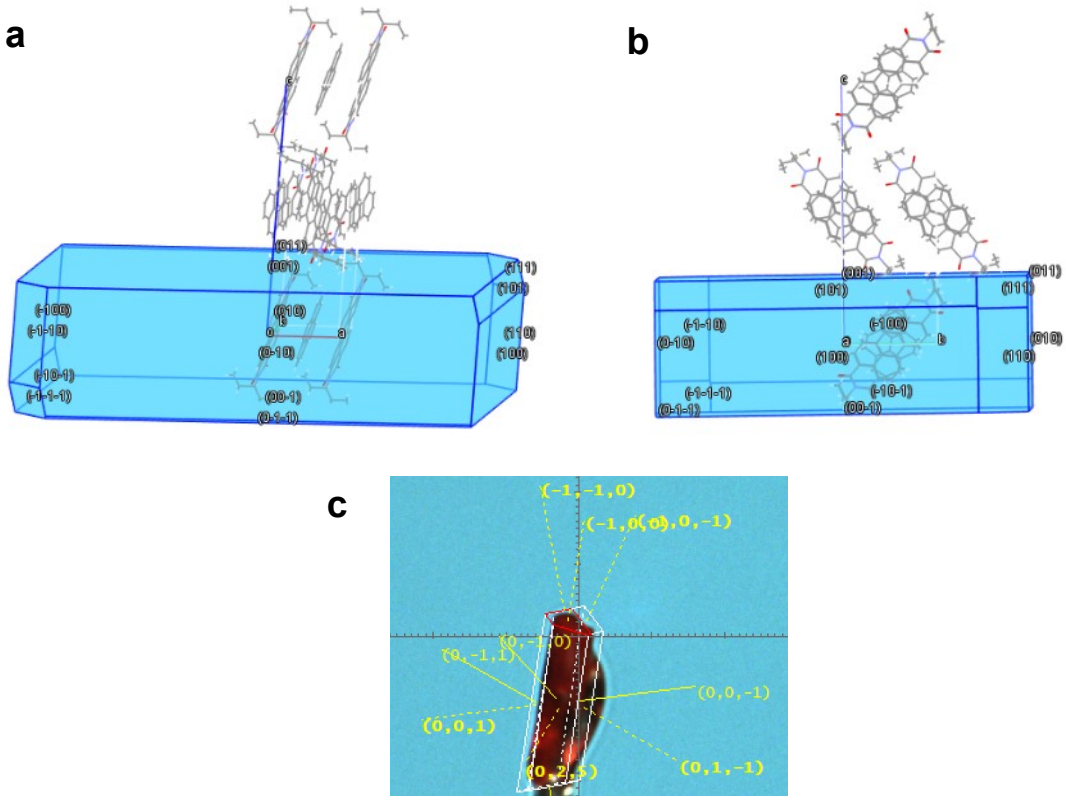

Figure S2: BFDH calculations were completed in Mercury for Pyr-C_5PDI co-crystal. (a) View of the crystal along the (010) axis shows the molecules stack with their transition dipole moments perpendicular to the long axis of the crystal. (b) View of the crystal along the (100) axis shows cleanly segregated stacks, with the planes of the molecules perfectly cofacial with the axis of the crystal. (c) Manual face indexing of the mounted single crystal that was diffracted shows reasonable agreement with the BFDH calculated structures.

Section 2: Steady-state Absorption and Emission Microscopy

Steady-state absorption spectra on the single crystals were obtained using an adapted commercial epi-illumination microscope (Nikon Ti-U) using the white light continuum probe beam from the femtosecond apparatus (see below). The white light source was focused on the sample with a 60× objective lens (Nikon, NA= 0.70), and the transmitted light was collected and recollimated with another 50× objective lens (Nikon, NA= 0.55) mounted over the sample. The collimated output was directed to a home-built spectrometer and the spectrally dispersed signal was recorded with a fast line-scan camera (OctoPlus, Teledyne e2v). To obtain an absorption spectrum, a reference transmission was first taken with the beam focused on the bare glass substrate, and the signal transmission was measured on the single crystal. The polarization of the beam was controlled with a broadband half-wave plate (HWP) before the microscope to obtain the steady-state absorption spectra at different polarizations.

Steady-state emission spectra were measured using a similar epi-illumination microscope (Nikon Ti-U), excited by a 532 nm continuous-wave laser (Spectra-Physics) beam. A 40× magnification objective lens (Nikon, NA = 0.60) was used both to focus the incident beam onto a single crystal and to collect the emitted light. The emitted light was then sent into an Acton spectrograph (Princeton Instruments) equipped with a PIXIS 400BR CCD Camera (Princeton Instruments). A long-pass filter was used to block the scattered excitation beam within the signal.

Polarized Absorption Plots.

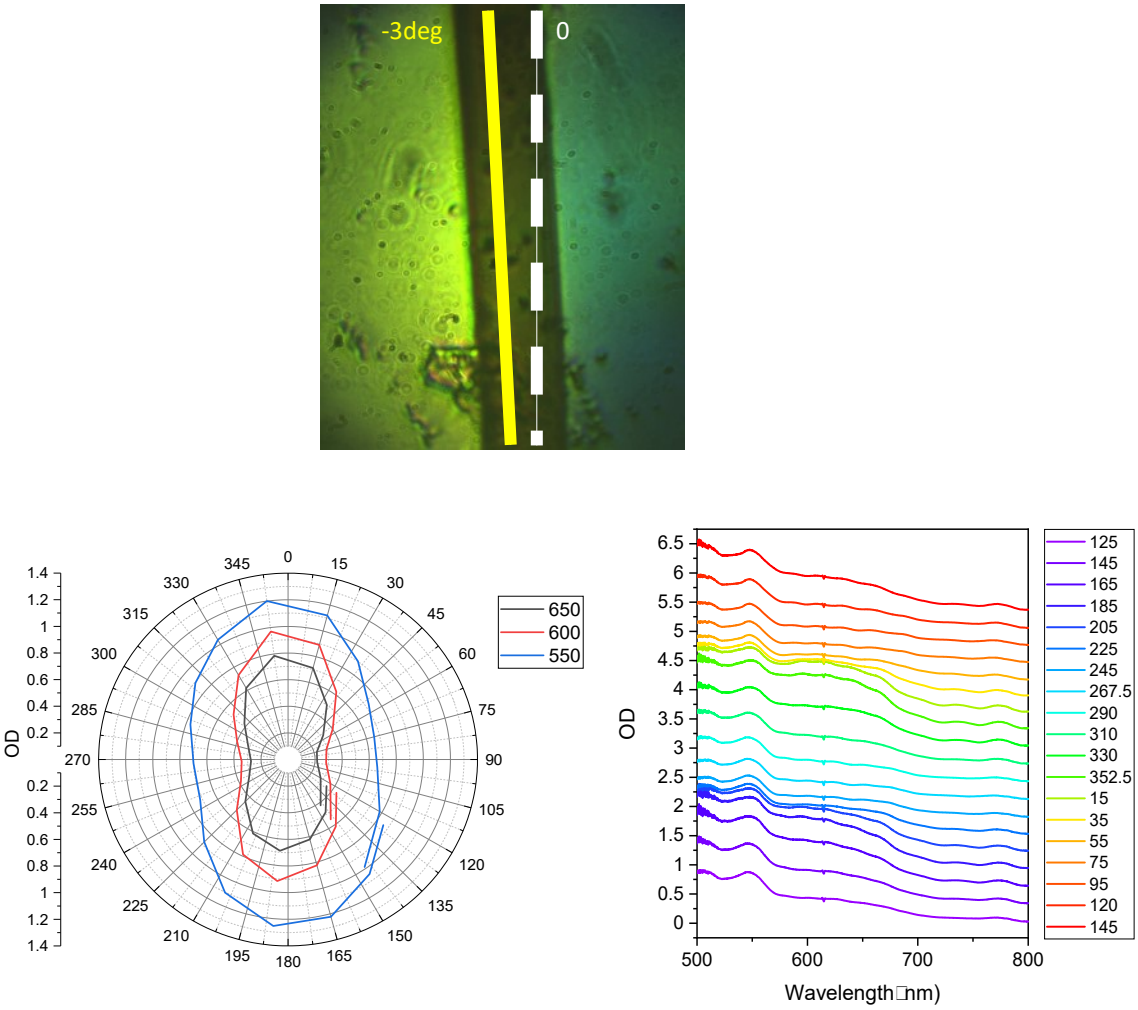

Figure S3a: Pyr-diisoPDI measured with probe at various polarizations.

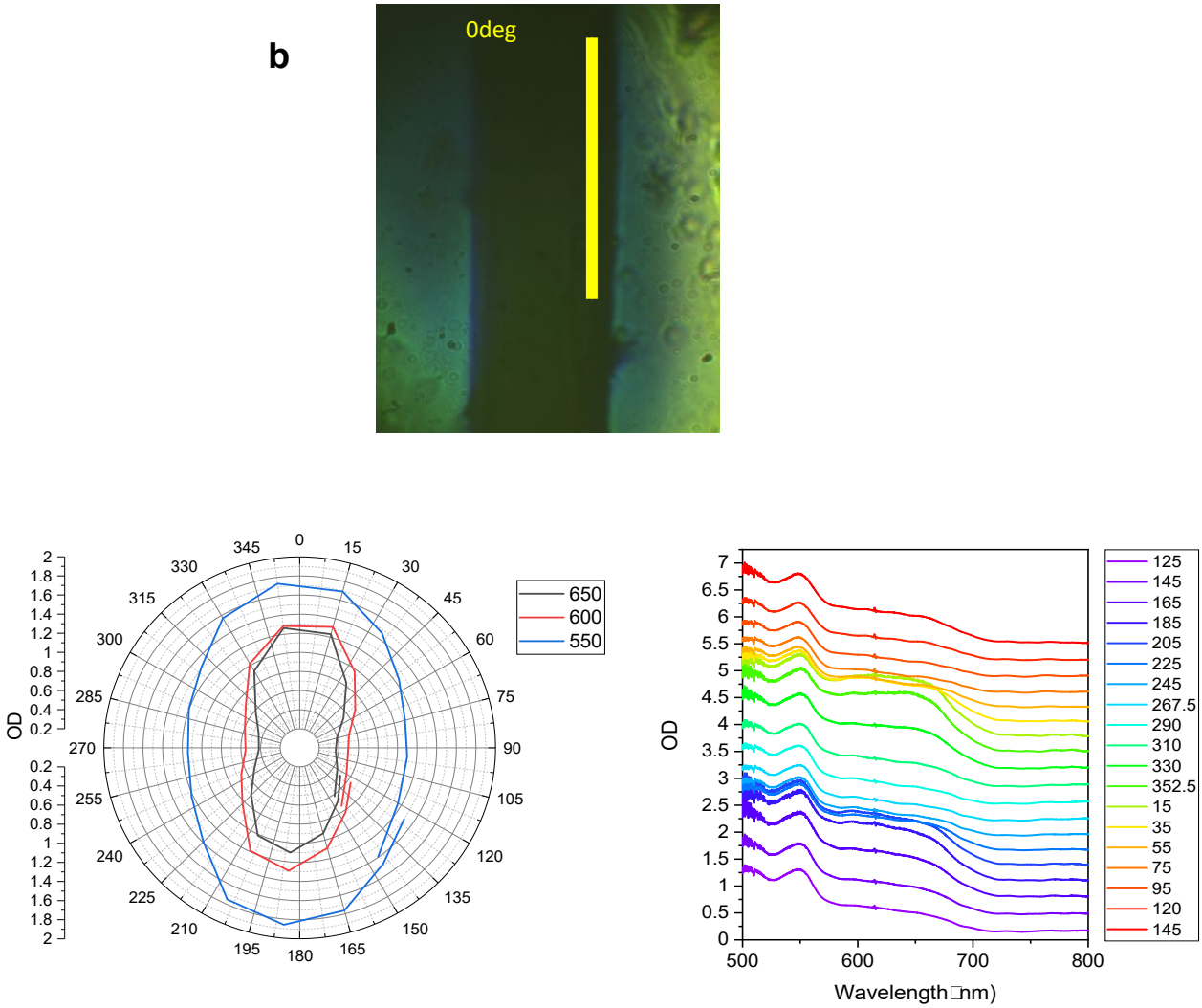

Figure S3b: Pyr-diisoPDI measured with probe at various polarizations.

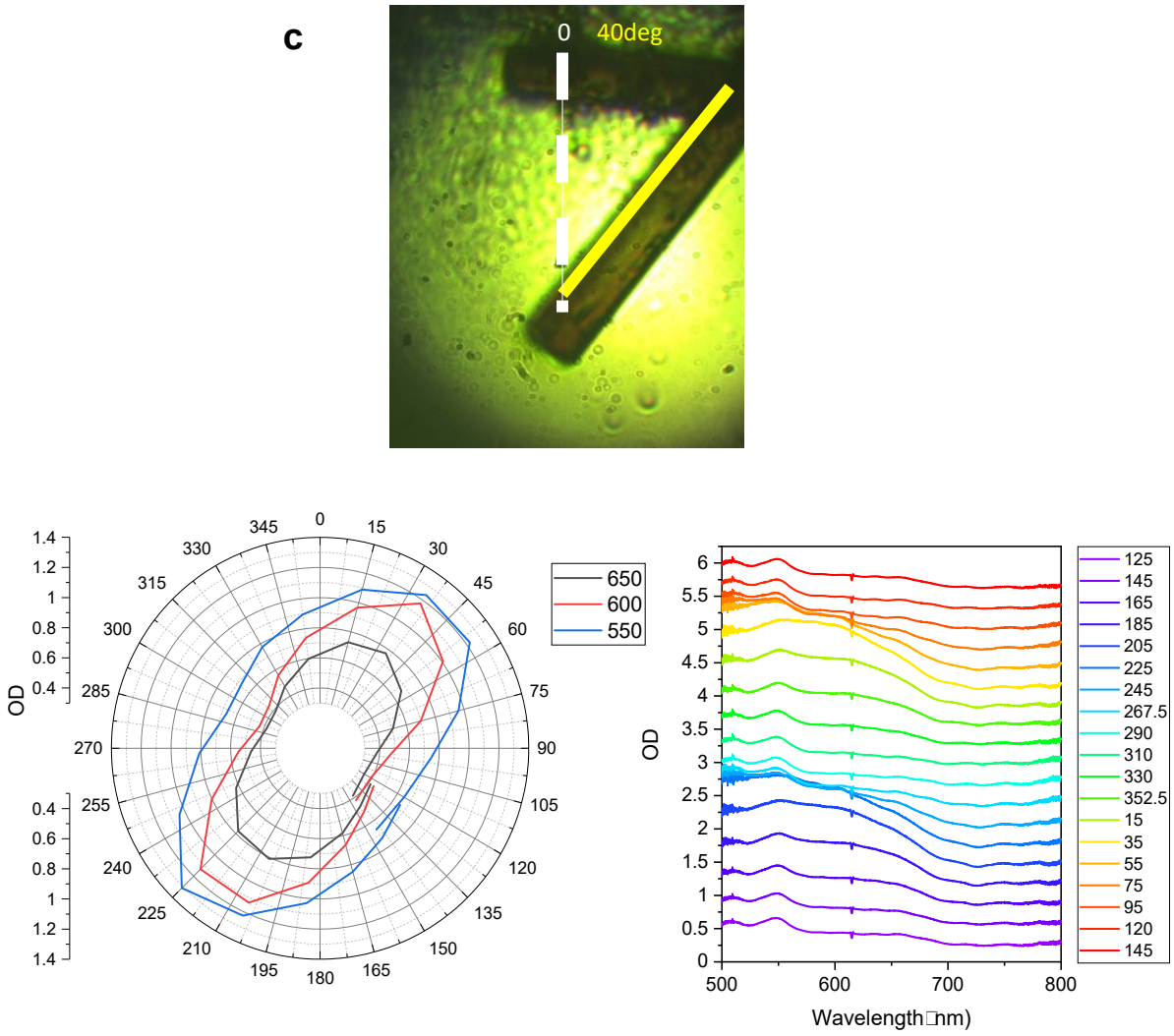

Figure S3c: Pyr-diisoPDI measured with probe at various polarizations.

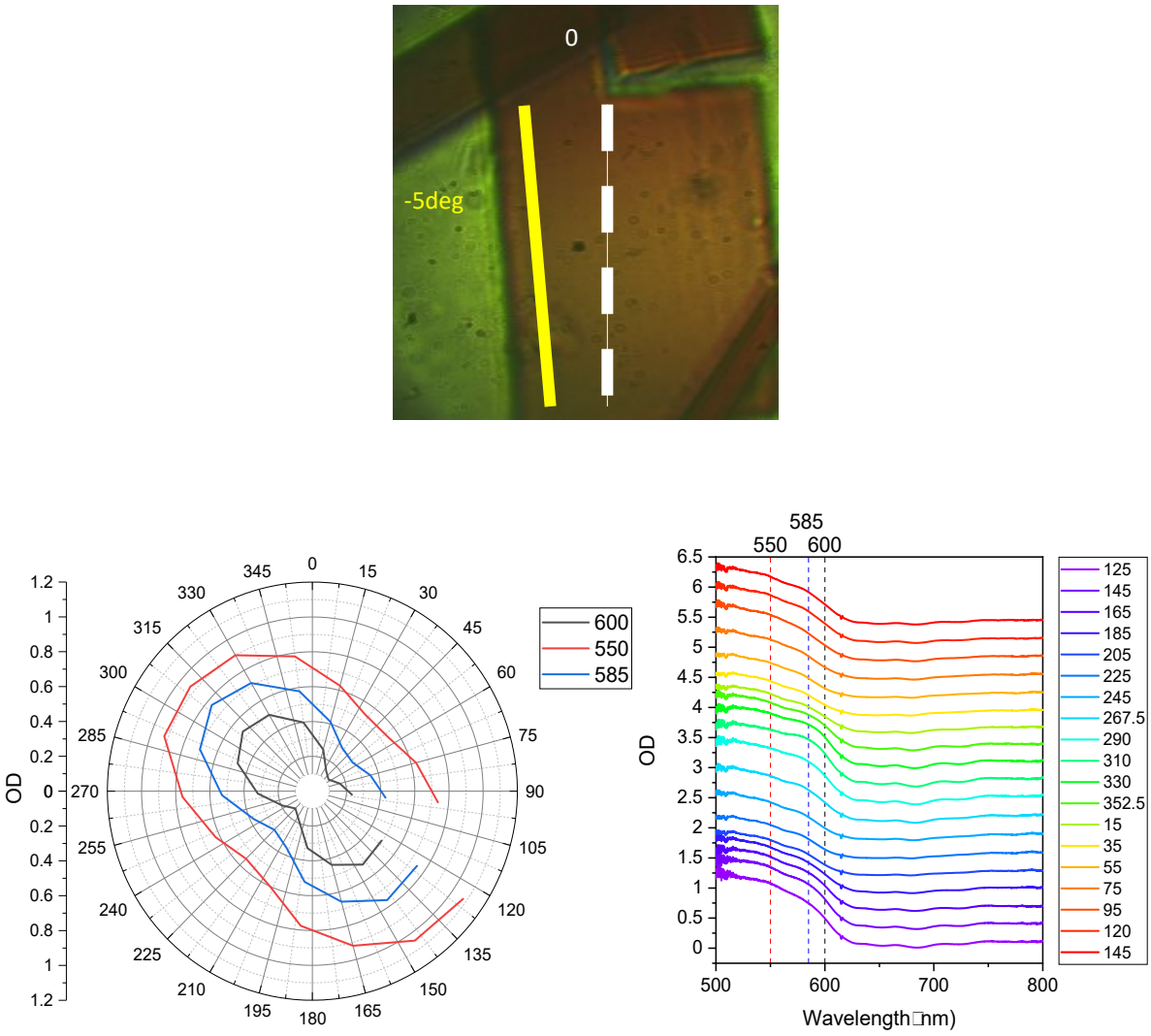

Figure S4a: Pyr-C_5PDI measured with probe at various polarizations.

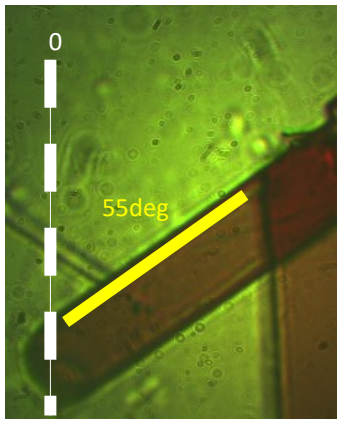

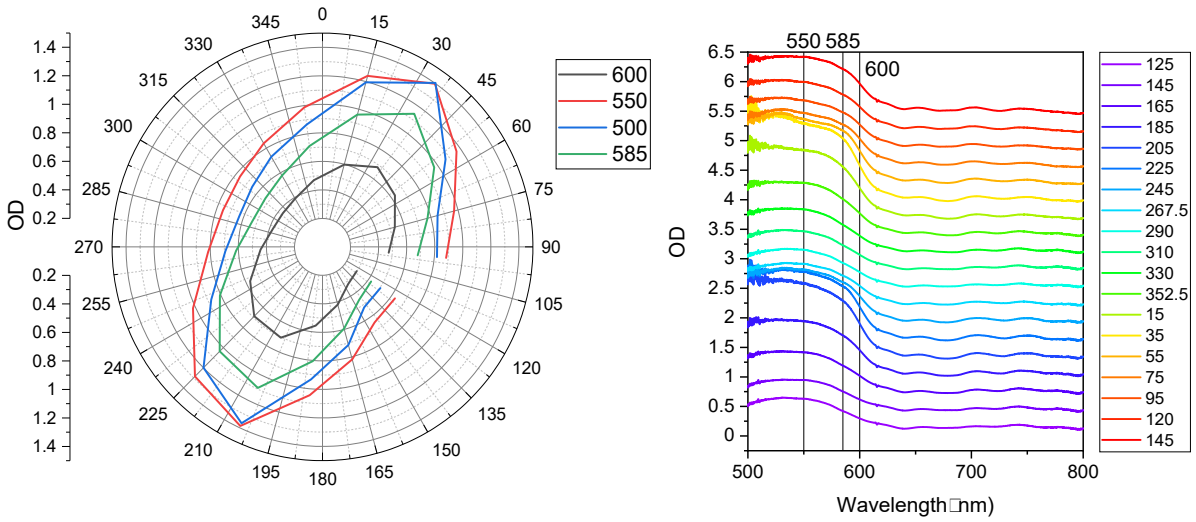

Figure S4b: Pyr-C_5PDI measured with probe at various polarizations.

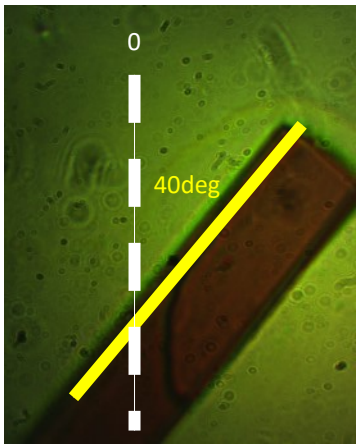

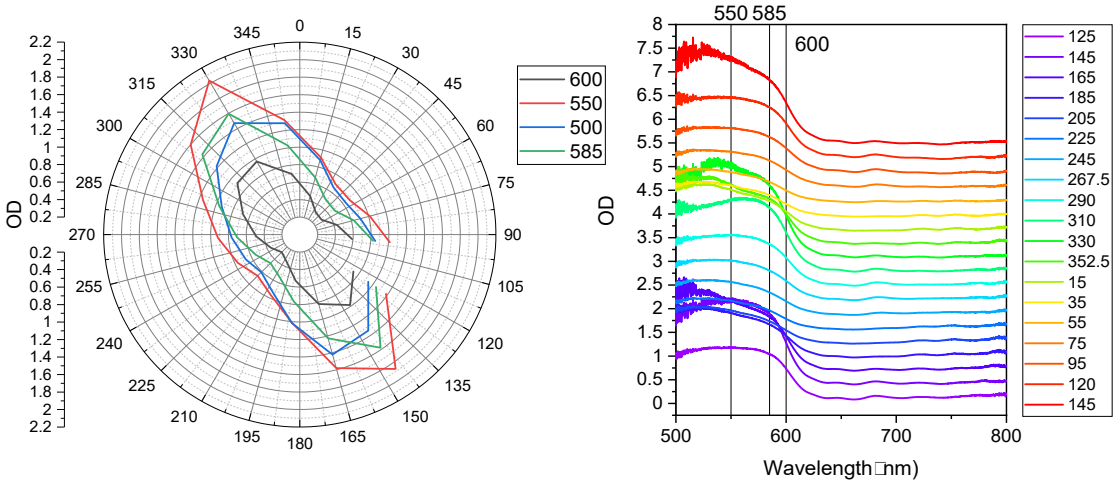

Figure S4c: Pyr-C_5PDI measured with probe at various polarizations.

Section 3: Femtosecond Transient Absorption Microscopy

Femtosecond transient absorption microscopy (fsTAM) was performed as follows: The 1040 nm fundamental output (> 8 W, < 400 fs, 200 kHz repetition rate) of a commercial amplified laser system (Spirit One, Spectra-Physics) was down-counted to 100 kHz with the integrated pulse picker, and then divided with a beam splitter (BS) into two beam paths. One beam (probe path) was sent to a double-pass linear delay line, and then focused into a 10 mm thick undoped yttrium aluminum garnet (YAG) crystal for white light continuum generation. The other fraction of the 1040 nm fundamental beam was used to drive a collinear optical parametric amplifier (Spirit-OPA-8, Spectra-Physics), which generated the visible pump pulses. The visible pump pulses were modulated at 50 kHz with an electro-optic amplitude modulator (EOAM-NR-C4, Thorlabs), which was synchronized to the fundamental laser output. The pump was converted to a circularly polarized beam before entering the modulator, and the modulated output pump beam was routed through a linear polarizer. This is followed by dispersion compensation of the modulated pump pulses using a prism compressor consisting of two prisms. The pump and probe beams were co-axially combined using a 50:50 BS and sent into the same microscope setup, spectrometer, and camera used for steady-state absorption measurements described above. The polarizations of the pump and the probe beams were controlled independently using two HWPs. The pump and probe focused spot sizes (FWHM) on the sample were 0.83 μm and 0.93 μm, with Gaussian beam shapes (Figure S5). The total instrument response function (IRF) was 400-600 fs.

Pump and probe spot sizes.

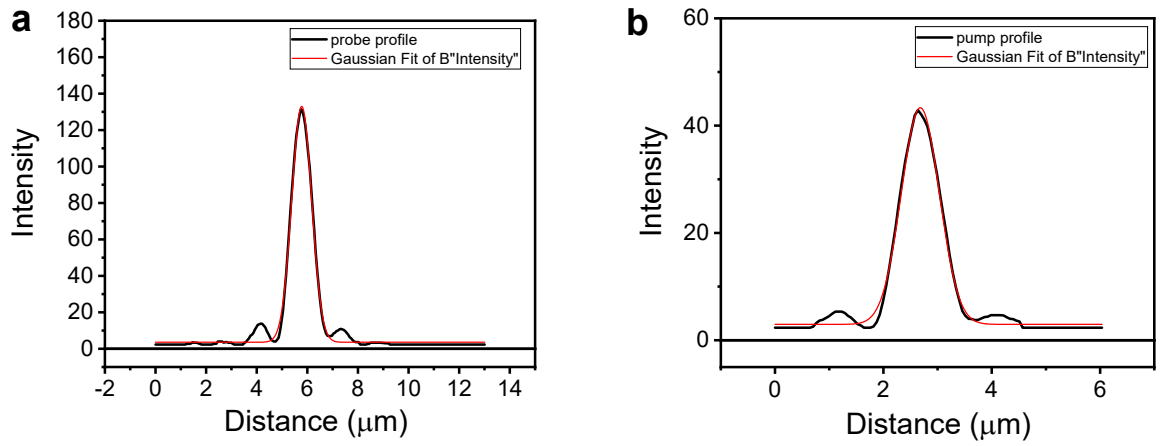

Figure S5: Gaussian fits for (a) probe and (b) pump spot sizes. Objective lens: Nikon (Plan fluor, ELWD, 60X/0.7)

Section 4: Calculation of excitation density

$$\xi = \frac{N_p}{V} = \frac{\lambda \times P \times (1 - 10^{-A})}{h \times c \times f \times \pi r^2 t}$$

Table S1:

λ (nm)	P (μW)	A (OD)	f (kHz)	r (μm)	t (μm)
540	17	0.25	50	0.46	2

The excitation density is the number of photons (N_p) in the excitation volume (V) per pulse. The values λ, P, A, f, r, t are the excitation wavelength, pump power, absorbance at the excitation wavelength, pump repetition rate, radius of the probe beam, and thickness of the crystal. Values h and c are Planck's constant and the speed of light in a vacuum. For the experiment at these parameters the excitation density is: 3.04×10^{20} cm^{-3}.

Section 5: Calculation of diffusion coefficients

To calculate the bimolecular rate constant, the data were fit to either one of the following kinetic models:

1. CT excitons annihilate through one-dimensional diffusion:

$$\frac{d[CT]}{dt} = k_2[CT]^2 \qquad (1)$$

Where $[CT]$ is the concentration of CT excitons and $k_2$is the rate coefficient of diffusion-controlled CT biexciton annihilation. Assuming one-dimensional diffusion of CT excitons and that annihilation is effectively instantaneous upon contact, k_2 may be related to the one-dimensional diffusion coefficient D_{1D}, annihilation radius R_{1D} of CT excitons, and the average molecular density throughout the system N_0 by[4]:

$$k_2 = \frac{1}{R_{1D}N_0}\sqrt{\frac{8D_{1D}}{\pi t}} = \frac{C}{\sqrt{t}}, C = \frac{1}{R_{1D}N_0}\sqrt{\frac{8D_{1D}}{\pi}} \qquad (2)$$

With N_0 calculated by:

$$N_0 = \frac{\rho \times N_A}{M_w} \qquad (3)$$

where ρ is the density of the unit cell, N_A is Avogadro's number, M_w is the molecular weight of the unit cell.

Solving the differential equation (1) with k_2 expressed as (2) yields[5]:

$$[CT] = \left([CT]_0^{-1} + 2C\sqrt{t}\right)^{-1} \qquad (4)$$

$[CT]_0$ is the initial concentration of CT excitons after excitation.

With TAM spectra, the concentration of CT excitons [CT] at any given time *t* after can be expressed by:

$$[CT] = \frac{\Delta OD}{\Delta OD_0} \times [CT]_0 \qquad (5)$$

Where ΔOD and ΔOD_0 are the TAM signal at time *t* and at time zero, respectively. Assuming every photon absorbed by the system converts to a CT exciton, $[CT]_0$ reduces to the excitation density ξ. The expression for ξ is:

$$\xi = \frac{N_p}{V} = \frac{\lambda \times P \times (1 - 10^{-A})}{h \times c \times f \times \pi r^2 t} \quad (6)$$

λ is the excitation wavelength, P the pump power, f the repetition rate, r the spot radius, t the thickness, and *A* the absorbance at the excitation wavelength and polarization as measured with steady-state absorption microscopy.

Plugging eqns (5) and (6) into (4), the evolution of TAM signal ΔOD can be expressed as:

$$\Delta OD = (\Delta OD_0{}^{-1} + \frac{2\xi C}{\Delta OD_0}\sqrt{t})^{-1} \quad (7)$$

TAM spectrum at 540 nm was fitted to equation (7) to obtain the *C* value, and finally equation (2) can be solved for the value of D_{1D}:

$$D_{1D} = \left(\frac{C}{\pi R_\rho{}^2}\right)^2 \times \frac{\pi}{8} = \frac{k_2{}^2}{32\pi R_\rho{}^4} \quad (8)$$

2. CT excitons annihilate through one-dimensional diffusion with a first order decay:

$$\frac{d[CT]}{dt} = -k_1[CT] - k_2[CT]^2 \quad (9)$$

Where k_1 is the unimolecular rate coefficient associated with the first-order CT exciton decay and $k_2$is the rate coefficient of diffusion-controlled CT biexciton annihilation.

Following equation 2, the kinetic model is written as:

$$\frac{d[CT]}{dt} = -k_1[CT] - \frac{C}{\sqrt{t}}[CT]^2 \quad (10)$$

The analytical solution to equation 10 is:

$$[CT] = \frac{\sqrt{A} \times D \times e^{-At}}{\sqrt{A} + CD\sqrt{\pi} - CD\sqrt{\pi} \times erfc(\sqrt{At})} \quad (11)$$

where $D = [CT]_0$, $A = k_1$ and the evolution of TAM signal is:

$$[OD] = \frac{\sqrt{A} \times e^{-At} \times [OD]_0}{\sqrt{A} + C\xi\sqrt{\pi} - C\xi\sqrt{\pi} \times erfc(\sqrt{At})} \quad (12)$$

The diffusion coefficient was calculated in the same way as in the purely one-dimensional diffusion model from the best-fit parameter *C*, according to eqns 4-8.

References

1. Sheldrick, G. M., Crystal structure refinement with shelxt. *Acta Crystallogr A* **2015,** *71*, 3-8.

2. Dolomanov, O. V.; Bourhis, L. J.; Gildea, R. J.; Howard, J. A. K.; Puschmann, H., Olex2: A complete structure solution, refinement and analysis program. *J. Appl. Crystallogr.* **2009,** *42*, 339-341.

3. Sheldrick, G. M., A short history of shelx. *Acta Crystallogr A* **2008,** *64*, 112-122.

4. Hudson, R. J.; Huang, D. M.; Kee, T. W., Anisotropic triplet exciton diffusion in crystalline functionalized pentacene. *J. Phys. Chem. C* **2020,** *124*, 23541-23550.

5. Markovitsi, D.; Lecuyer, I.; Simon, J., One-dimensional triplet energy migration in columnar liquid crystals of octasubstituted phthalocyanines. *J. Phys. Chem.* **1991,** *95*, 3620-3626.